Ab initio calculation of charge-transfer and excitation cross sections in $Li^+ + H(1s)$ collisions

L. F. Errea,[1] F. Guzmán,[1,2] L. Méndez,[1] B. Pons,[3] and A. Riera[1]
[1]*Laboratorio Asociado al CIEMAT de Física Atómica y Molecular en Plasmas de Fusión, Departamento de Química C IX, Universidad Autónoma de Madrid, Cantoblanco E-28049 Madrid, Spain*
[2]*Laboratorio Nacional de Fusión por Confinamiento Magnético, CIEMAT, E-28040, Madrid, Spain*
[3]*CELIA (UMR CNRS), Universitè de Bordeaux I, 33405 Talence Cedex, France*
(Received 10 October 2007; published 9 January 2008)

We present total charge transfer for $H^+ + Li$ collisions and total and state-selected cross sections for charge transfer and excitation in $Li^+ + H$ collisions in the energy range 25–2500 eV/amu. The calculation employs quantal and semiclassical treatments and a molecular expansion in terms of both *ab initio* and model potential orbitals. Isotopic dependence of $Li^+ + H$ charge-transfer cross section is studied.

DOI: 10.1103/PhysRevA.77.012706 PACS number(s): 34.10.+x, 34.70.+e

I. INTRODUCTION

Collisions involving Li and Li^+ are important processes in controlled fusion because the first wall of some devices [1,2] is coated with liquid lithium in order to reduce sputtering. The interaction of Li atoms with the plasma constituents yields Li^+, and the charge transfer (CT) between this impurity and hydrogen can take place in the plasma edge. In addition, since this CT process yields excited Li, the ensuing emission could provide a diagnostic tool. However, to our knowledge, only the experiment of Shah *et al.* [3] has considered this process, at energies higher than 5 keV/amu. In the present work we have evaluated total and partial cross sections for the CT reaction:

$$^7Li^+(1s^2) + H(1s) \rightarrow {}^7Li(1s^2nl) + H^+ \tag{1}$$

and the excitation process

$$^7Li^+(1s^2) + H(1s) \rightarrow {}^7Li^+(1s^2) + H(nl). \tag{2}$$

The inverse CT reaction:

$$^7Li(1s^22s) + H^+ \rightarrow {}^7Li^+(1s^2) + H(nl) \tag{3}$$

has been studied in several works (see Ref. [4], and references therein) because fast ($E > 10$ keV) neutral Li beams are employed in charge exchange diagnostics [5,6]; thus, previous studies have focused on relatively high collision energies ($E > 0.5$ keV/amu) but measurements and calculations at low energies have not been carried out. In the present work we have calculated total and partial cross sections for reactions (1)–(3) in the energy range 25 eV/amu $< E < 2.5$ keV/amu; these calculations have been performed using a molecular expansion and semiclassical and quantal dynamical treatments. As in our recent work [7], we have employed quantal and semiclassical methods in order to accurately evaluate the cross sections in a large energy range, as required in the applications.

A critical issue in the development of future fusion devices as the International Thermonuclear Experimental Reactor (ITER) is the minimization of tritium inventory, so that, atomic data involving this isotopic species are required. In this respect, semiempirical formulas have been proposed for estimating the isotopic dependence of CT cross sections for some collision systems [8]. Nevertheless, these expressions are adequate for reactions taking place through transitions in avoided crossings between the potential energy curves at large internuclear separations. As we shall explain in detail in Secs. III and IV, the first stage of the mechanism of reactions (1) and (2) are transitions at very short internuclear distances, and therefore we have carried out cross section calculations with deuterium (D) and tritium (T).

The paper is organized as follows. In Sec. II we summarize the methods employed in the calculation. In Sec. III we present the electronic energies and dynamical couplings between the molecular wave functions. Our results are presented in Sec. IV. In this section we start by comparing our results for reaction (3) with previous calculations and experimental results, which allow us to check the convergence of the molecular expansion, and in particular to settle the high-energy bound of this expansion. Our main conclusions are outlined in Sec. V.

II. DYNAMICAL TREATMENT

The methods employed in the dynamical calculation have been explained in detail in previous publications (see Ref. [7], and references therein) and will be only summarized here. In the semiclasical eikonal treatment (see Ref. [9]), the internuclear distance $\boldsymbol{R}$ follows a rectilinear trajectory $\boldsymbol{R} = \boldsymbol{b} + \boldsymbol{v}t$ and the electronic motion is described quantally by means of the wave function $\Psi^{SC}(\boldsymbol{r},t;b,v)$, solution of the semiclassical equation

$$\left[H_{el}(\boldsymbol{r},\boldsymbol{R}) - i \left.\frac{\partial}{\partial t}\right|_{\boldsymbol{r}} \right] \Psi^{SC}(\boldsymbol{r},t;b,v) = 0, \tag{4}$$

where H_{el} is the clamped-nuclei electronic Hamiltonian in the Born-Oppenheimer approximation. The wave-function Ψ^{SC} is expanded in the molecular basis set ϕ_k in the form

$$\Psi^{SC}(\boldsymbol{r},t;b,v) = D(\boldsymbol{r},t) \sum_k a_k(t;b,v)\phi_k(\boldsymbol{r},\boldsymbol{R}) \times \exp\left[-i \int_0^t \epsilon_k(R)dt \right], \tag{5}$$

where ϵ_k are the energies of the MOs and D is a common translation factor (CTF) [10], which is introduced to ensure

that the truncated expansion fulfills the asymptotic conditions. Substitution of the expansion (5) in Eq. (4) leads to the system of differential equations

$$i\frac{da_j}{dt} = \sum_k \langle \phi_j D|H_{\rm el} - i\frac{\partial}{\partial t}|\phi_k D\rangle a_k \times \exp\left\{-i\int_0^t [\epsilon_k(R) - \epsilon_j(R)]dt\right\} \tag{6}$$

which is numerically solved to yield the probability for the $i \to k$ transition, for given v and b:

$$P^k(b,v) = \lim_{t\to\infty} |\delta_{ik} - a_k(t;b,v)|^2 \tag{7}$$

and corresponding cross sections

$$\sigma^k(v) = 2\pi \int_0^\infty bP^k(b,v)db. \tag{8}$$

At low energies we have applied a quantal treatment where the collision wave function is a solution of the Schrödinger equation

$$H\Psi^{\rm Q}(\boldsymbol{r},\boldsymbol{R};J,\mathcal{E}) = \mathcal{E}\Psi^{Q}(\boldsymbol{r},\boldsymbol{R};J,\mathcal{E}) \tag{9}$$

where $H = -\frac{1}{2\mu}\nabla_R^2 + H_{\rm el}$ is the nonrelativistic Hamiltonian for the collision system, $\mathcal{E}$ is the center of mass energy, and μ the nuclear reduced mass. In the quantal calculation we have employed the common reaction coordinate method [11] to ensure that the expansion fulfills the asymptotic conditions. In this treatment the collision wave function is expanded, for each value of the angular momentum J, in terms of the molecular wave functions

$$\Psi^{Q}(\boldsymbol{r},\boldsymbol{\xi};J,\mathcal{E}) = \sum_k F_k(\xi,J,\mathcal{E})\phi_k(\boldsymbol{r},\boldsymbol{\xi};J,\mathcal{E}), \tag{10}$$

where $\xi(\boldsymbol{r},\boldsymbol{R})$ is the common reaction coordinate.

The cross sections are given by

$$\sigma^k(\mathcal{E}) = \frac{2\pi}{k_i^2}\sum_J (2J+1)|\delta_{ik} - S_{ik}(J,\mathcal{E})|^2 \tag{11}$$

with k_i the initial momentum. The S matrix is evaluated from the radial functions F_k, which are calculated by solving numerically the system of differential equations obtained by substituting the expansion (10) in the Schrödinger Eq. (9).

In our calculation the CTF and the reaction coordinate are defined in terms of the same switching function, and we have employed the form suggested in Ref. [12]:

$$f(\boldsymbol{r}_i,\boldsymbol{R}) = \frac{R^2}{R^2+\beta^2}\boldsymbol{r}_i \cdot \hat{\boldsymbol{R}} \tag{12}$$

which has been employed in almost all calculations in terms of *ab initio* molecular functions (see, e.g., Ref. [13]). In both formalisms the coupling terms proportional to v are the modified radial and rotational couplings of the form

$$R_{jl} = \langle \phi_j|\frac{\partial}{\partial R}|\phi_l\rangle + \left[\frac{R}{R^2+\beta^2} - R\left(\frac{R}{R^2+\beta^2}\right)^2\right] \times \langle \phi_j|\sum_{\alpha=1}^N z_\alpha \frac{\partial}{\partial z_\alpha}|\phi_l\rangle, \tag{13}$$

$$L_{jl} = \langle \phi_j|\sum_{\alpha=1}^N L_y(\alpha)|\phi_l\rangle + \frac{R}{R^2+\beta^2}\langle \phi_j|\sum_{\alpha=1}^N \left(z_\alpha\frac{\partial}{\partial x_\alpha} + x_\alpha\frac{\partial}{\partial z_\alpha}\right)|\phi_l\rangle, \tag{14}$$

where x_α and z_α are the electronic coordinates in the molecular reference frame, where $\hat{Z}=\hat{R}$ and $\hat{Y}$ is perpendicular to the collision plane $(\hat{X},\hat{Z})$. We must note that in the eikonal calculations we have also included the terms proportional to v^2 coming from the translation factor.

III. MOLECULAR DATA

In the molecular calculation we have employed the MELDF code (Quantum Chemistry Program Exchange, QCPE Program No. 580, see, e.g., Ref. [14]). We have generated a set of molecular orbitals (MOs), $\{\phi_j\}$ by carrying out a restricted Hartree-Fock calculation for the two-electron system LiH^{2+}; this yields the occupied (core) orbital ϕ_1 and a set of virtual orbitals, which are approximations to those of the three-electron system LiH^+. We have applied the frozen core approximation where the core orbital is doubly occupied and therefore the molecular wave functions with $M_S = \pm\frac{1}{2}$ are $\|\phi_1\bar{\phi}_1\phi_j\|$, $\|\phi_1\bar{\phi}_1\bar{\phi}_j\|$, respectively. In our calculation, the MOs are linear combinations of a two-center Gaussian basis set; it includes $(13s\ 10p\ 5d\ 5f)$ Cartesian Gaussian orbitals centered on the Li nucleus, contracted to $[5s\ 3p\ 2d\ 1f]$ functions, and $(13s\ 8p\ 5d)$ on the H nucleus contracted to $[5s\ 4p\ 2d]$ [28]. To check the accuracy of this basis we have compared our calculated energy differences in the limit $R \to \infty$ with the experimental ones [15] and we have found differences smaller than 5×10^{-3} hartree. We have obtained the MOs for $R > 0.1a_0$ (the basis set becomes linearly dependent at smaller R). As an additional test, we have extrapolated the MO energies to $R \to 0$, and checked that the differences with the spectroscopic values for Be^+ were also smaller than 5×10^{-3} hartree for s and p levels, and about 2×10^{-2} hartree for d levels, probably because the relatively small number of Gaussian d functions in our basis.

In Fig. 1 we show the energies of the 17 MOs (σ and π) included in the dynamical calculation. In this figure we have not plotted the energy of the core orbital ϕ_1 and we have divided the figure in two panels with different energy scales to show more clearly the energies of the excited orbitals. To help with the discussion of the collision mechanism, we have listed in Table I the adiabatic limit of the MOs as $R \to \infty$.

In order to compare with previous works, and as an additional check of the accuracy of the *ab initio* calculation, we present in Fig. 2 the comparison of the orbital energies of the σ MOs with those obtained from a model potential calcula-

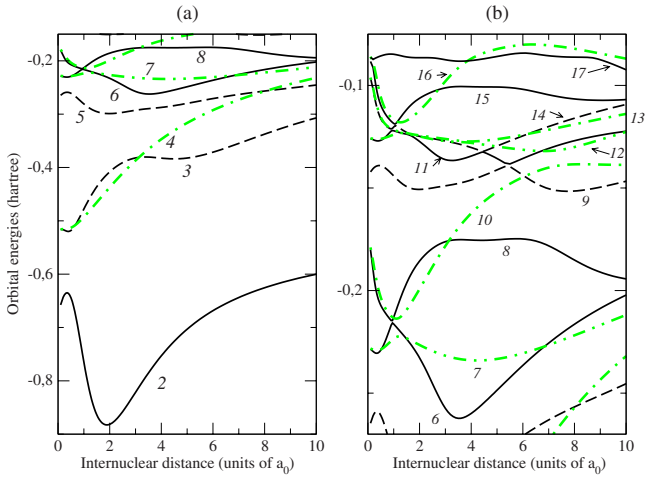

FIG. 1. (Color online) Energies of the orbitals of the LiH^+ quasimolecule as functions of the internuclear distance. —: σ orbitals dissociating into $Li^+ + H$; $-\cdots-$: π orbitals dissociating into $Li^+ + H$; $- - -$: σ orbitals dissociating into $Li + H^+$; $-\cdot-\cdot-$: π orbitals dissociating into $Li + H^+$.

tion where the MOs are the eigenfunctions of the one-electron Hamiltonian

$$h = -\frac{1}{2}\nabla^2 - \frac{1}{r_H} + V_{mod}(r_{Li}) \tag{15}$$

and

$$V_{mod}(r_{Li}) = -\frac{1}{r_{Li}} - \frac{2}{r_{Li}}(1 + \alpha r_{Li})\exp(-2\alpha r_{Li}), \tag{16}$$

where r_{Li}, r_H are the electronic distances to the nuclei and the parameter $\alpha = 1.655$ has been obtained by fitting the ionization potential of the lithium atom; this model potential is similar to that employed in Refs. [16] and [17]. We have also compared in Fig. 2 the *ab initio* orbital energies with those obtained from the three-parameter model potential proposed by Klapisch [18]:

TABLE I. Correlation of the MOs in the limit $R \to \infty$. The MOs are labeled as in Fig. 1.

MO	Dissociation limit
ϕ_1	$Li(1s) + H^+$
ϕ_2	$Li^+ + H(1s)$
ϕ_3	$Li(2s) + H^+$
ϕ_4, ϕ_5	$Li(2p) + H^+$
ϕ_6, ϕ_7, ϕ_8	$Li^+ + H$ $(n=2)$
ϕ_9	$Li(3s) + H^+$
ϕ_{10}, ϕ_{14}	$Li(3p) + H^+$
ϕ_{13}, ϕ_{18}	$Li(3d) + H^+$
ϕ_{11}, ϕ_{12}, ϕ_{15}, ϕ_{16}, ϕ_{17}	$Li^+ + H$ $(n=3)$

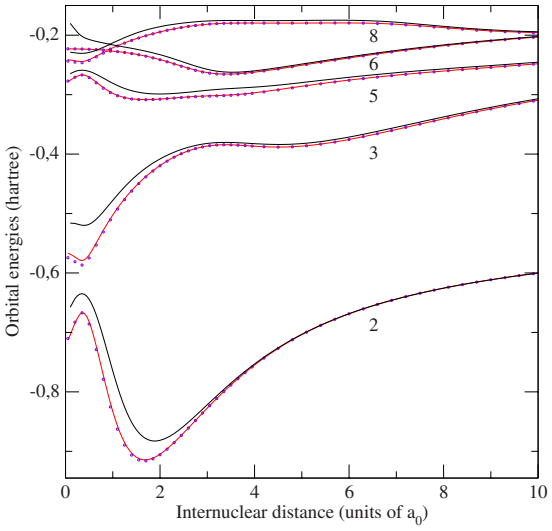

FIG. 2. (Color online) Comparison of *ab initio* (—) and model potential orbital energies [—: Eq. (16), ●: Eq. (17)] of the σ orbitals dissociating into $Li^+ + H$ $(n=1,2)$ and $Li(2l) + H^+$.

$$V^k_{mod}(r_{Li}) = -\frac{1}{r_{Li}} - \frac{[(Z-1)e^{-\gamma_1 r_{Li}} + \gamma_2 r_{Li} e^{-\gamma_3 r_{Li}}]}{r_{Li}} \tag{17}$$

with $\gamma_1 = 7.908\,75$, $\gamma_2 = 10.321$, and $\gamma_3 = 3.900\,06$. Good agreement can be noted the between both approximations except for $R < 2.0a_0$, where the delocalization of the MO ϕ_1 of the *ab initio* calculation, which cannot be described by the one-center model potential, starts to be sizeable. In this respect, the comparison of the energy levels of Be^+ with those of the united atom limit of the model potential MOs (Fig. 2) shows that this approach is not accurate in this limit.

The dynamical couplings have been evaluated numerically as explained in Ref. [19]. The most relevant couplings are shown in Fig. 3(a). The main mechanism of the CT reaction (1) at low energies involves in a first stage the transition $\phi_2 - \phi_3$ in the neighborhood of the pseudocrossing between the corresponding energies at $R \simeq 0.35a_0$ [see Figs. 1(a) and 3(a)]. Since the depopulation of the entrance channel takes place through transitions at short internuclear distances, a relatively small CT total cross section is expected for this reaction. The population of other CT and excitation

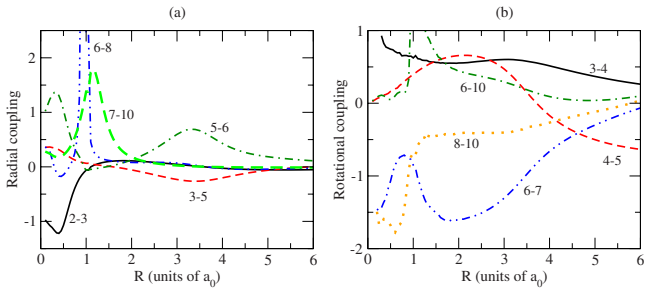

FIG. 3. (Color online) Radial [Eq. (13)] (a) and rotational [Eq. (14)] components (b) of the dynamical couplings between the lowest MOs. The MOs are labeled as in Fig. 1.

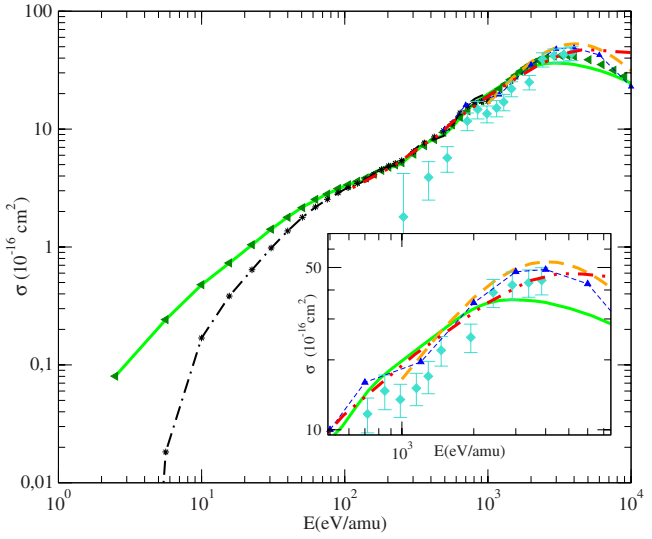

FIG. 4. (Color online) Cross sections for total charge-transfer H^++Li collisions. Present results: Calculations with the 17MO *ab initio* basis set. —: eikonal calculation basis set; –·–·: quantal calculation. Calculations with the 7MO *ab initio* basis set: ◀, eikonal calculation; *, quantal calculation. Previous calculations for total charge transfer: –▲–, results of Ref. [21]; -·-·, results of Ref. [17]. - - -, results of Ref. [4] for target electron loss. Experimental results: ◆ [20].

channels takes place through transitions from ϕ_3 to excited MOs; in particular, CT to Li$(2p)$+H^+ involves the rotational coupling between MOs ϕ_3 and ϕ_4, and the radial coupling in the broad avoided crossing between the energies of the orbitals ϕ_3 and ϕ_5. The channels dissociating into Li^++H $(n=2)$ are populated in a secondary process from the CT channels, namely, through the radial transition $\phi_5-\phi_6$. One can note the high peak of the radial coupling $\phi_6-\phi_8$ in Fig. 3(a) in the neighborhood of the avoided crossing at $R\simeq 0.9a_0$. This avoided crossing is also responsible for the changes of the rotational couplings 6-7, 6-10, and 8-10 [Fig. 3(b)] in the same region. At low energies, transitions to Li $(3s,3p)$+H^+ and Li^++H $(n=3)$ are unlikely, since they involve a multistep mechanism via the lower-lying orbitals.

IV. RESULTS AND DISCUSSION

A. Li+H^+ collisions

We have evaluated the total cross section for reactions (1)–(3) by using quantal and eikonal treatments and with two basis sets. The first basis set, called 7MO, includes the MOs $(\phi_2-\phi_8)$ dissociating into Li^++H $(n=1,2)$ and Li$(2l)$+H^+, and whose energies are plotted in Fig. 1(a). In the second basis set (17MO) we have added to the 7MO basis the σ and π MOs dissociating Li^++H $(n=3)$ and Li$(3l)$+H^+ (see Table I).

We present in Fig. 4 our values for the cross section of reaction (3) compared to previous experimental and theoretical results. We have plotted in this figure quantal and semiclassical results, which overlap over the energy range 150 – 1000 eV/amu. Our results show satisfactory agreement

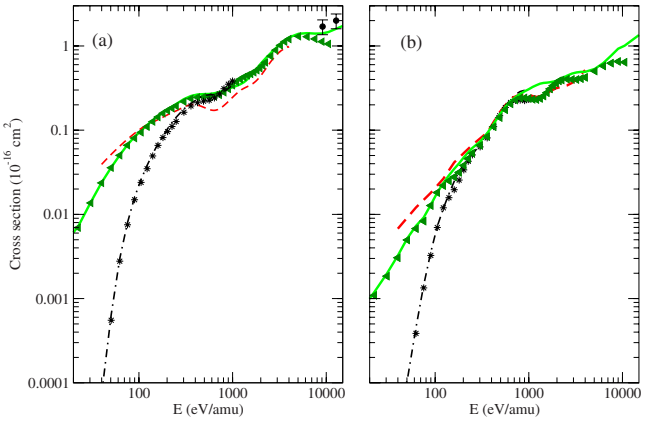

FIG. 5. (Color online) Total cross sections for charge-transfer (a) and H excitation (b) in Li^++H$(1s)$ collisions. Calculations with the 17MO *ab initio* basis set: —, eikonal calculation basis set; –·–·, quantal calculation. Calculations with the 7MO *ab initio* basis set: ◀, eikonal calculation; *, quantal calculation. - - -, eikonal calculation with the model potential 7MO basis set. ●, experimental results of Ref. [3].

with the experimental values of Varghese *et al.* [20], and, for $E<2.5$ keV/amu, with the calculations of Frisch and Lin [21], who employed an atomic orbital expansion that includes united atom orbitals. In this energy range, our results are practically identical to those of Salas [17], who applied a molecular expansion similar to ours with the MOs obtained from a model potential calculation, although a larger basis was included in that calculation. At $E>2.5$ keV/amu (see the inset of Fig. 4), the calculation of Ref. [17] starts to deviate from the atomic calculation of Ref. [21], where very excited atomic levels are populated. In addition, at $E>5$ keV, the difference of the results of Ref. [21] with the electron-loss cross sections of Schweinzer *et al.* [4] is the ionization cross section, which has been measured in Ref. [22]. Since our basis set and that of Ref. [17] do not include pseudostates, to represent the electronic continuum, both molecular expansions are not appropriate to evaluate the CT total cross section at these impact energies.

As a result of the comparison between our results and those of previous calculations, and given the good agreement between 17MO and 7MO results, we can conclude that the 17MO calculation is appropriate for energies below 2.5 keV/amu. Furthermore, since reactions (1) and (2) take place through transitions from the MO ϕ_2, while the entrance channel for reaction (3) is the MO ϕ_3, we expect smaller transitions to excited orbitals in the former case and therefore a faster convergence than for reaction (3).

B. Li^++H collisions

Our results for reactions (1) and (2) with eikonal and quantal treatments are plotted in Fig. 5. As expected, the eikonal method is not appropriate at low energies, although in the present system we find agreement between eikonal and quantal results at larger energies $(E>300$ eV/amu) than for other collisions [7,13,23]. The most important limitation of

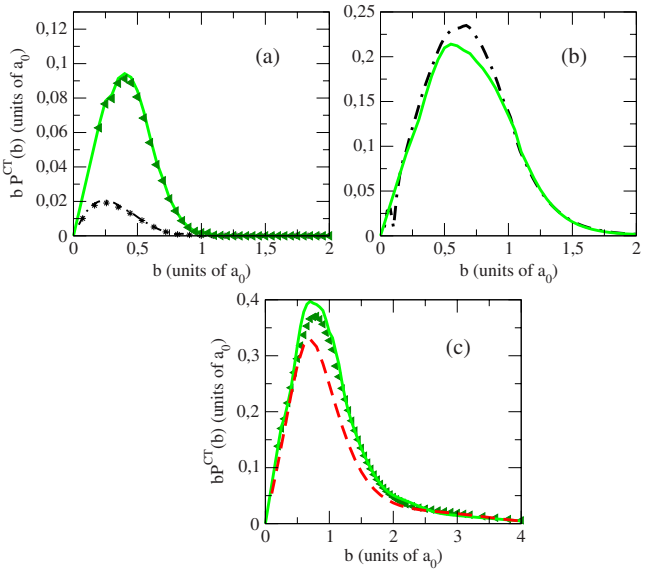

FIG. 6. (Color online) Product of the impact parameter b and the charge-transfer probability P^{CT} in $Li^+ + H(1s)$ at $E=100$ eV/amu (a), $E=1$ keV/amu (b), and $E=2.5$ keV/amu (c). Symbols as in Fig. 5.

the eikonal calculation comes from trajectory effects, as found in previous works (see Ref. [7], and references therein). An illustration of this point is shown in Fig. 6(a), where we plot the product of b and the charge-transfer probability P^{CT} as function of b for $E=100$ eV/amu. In order to compare quantal and classical calculations we employ the equivalence

$$[bP^j(b,E)]^Q = \left(\frac{2\pi}{k_i^2}\right)(2J+1)|\delta_{ij} - S_{ij}^J|^2 \qquad (18)$$

with $b^Q=(J+1/2)/k_i$. In Fig. 6(a) we find a very large difference between quantal [see Eq. (18)] and eikonal probabilities. These differences are easily understood if we take into account that at this energy, and for an impact parameter of $0.5a_0$, the distance of closest approach R_0 assuming a Coulomb interaction potential $1/R$ is $R_0 \simeq 0.7a_0$; so that the transition probability in the eikonal calculation comes mainly from transitions at internuclear separations that were inaccessible if the Coulomb distortion of the trajectory would be considered. The quantal calculation is, however, less accurate than the eikonal one at high impact energies because in this calculation we have neglected terms proportional to v^2 coming from the common reaction coordinate, as explained in Ref. [23]. To check this point we have performed eikonal calculations removing these terms, which point out that they introduce a significant variation of the cross section of Fig. 5 at $E>1$ keV/amu. At $E\simeq 1$ keV/amu, we obtain good agreement between quantal and semiclassical CT transition probabilities, as shown in Fig. 6(b).

The good agreement between total cross sections for reactions (1) and (2) calculated with the two bases (7MO and 17MO) at $E<3$ keV/amu (Fig. 5) indicates that the values obtained with the 17MO basis set has converged in this energy range, in agreement with our findings for reaction (3). At higher energies, the population of MOs dissociating into $Li(n=3)+H^+$ and $Li^+ + H(n=3)$ is not negligible, and we find significant differences in total cross sections and transition probabilities [see Fig. 6(c)]. An additional indication of the convergence of our basis set is provided by the comparison with the experimental results of Ref. [3]. In order to include these results we have extended the energy range in Fig. 5 up to $E=20$ keV. The agreement of our 17MO results with the experimental ones indicates that this basis set can be safely used below the energy limit (2.5 keV/amu) of the present calculation.

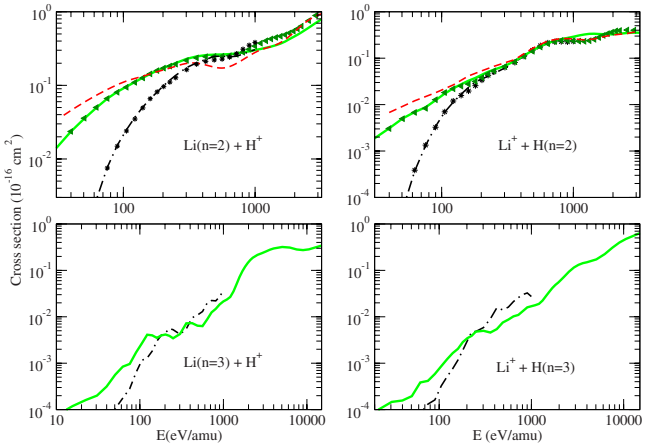

FIG. 7. (Color online) Cross sections for charge transfer into $Li(n=2,3)+H^+$ and H excitation to H $(n=2,3)$ in $Li^+ + H(1s)$ collisions, as indicated in the figure. Symbols as in Fig. 5.

On the other hand, the convergence of the molecular expansion depends in general on the functional form of the CTF. Although, for collisions where transitions take place at relatively large internuclear distances, changes in the form of the CTF do not appreciably modify the cross sections, when the main mechanism involves transitions at short R (a stringent example are $He^+ + H$ collisions [24,25]), the form of the CTF may be critical. Since the first step of reactions (1) and (2) is the transition $\phi_2 - \phi_3$ at $R \simeq 0.5a_0$, it is important to gauge the influence in the results of changes in the CTF. As a first test we have checked that the total cross sections do not appreciably change when the parameter β of Eq. (12) is modified around $\beta=3$, which are the optimal values obtained with the norm method [26]. In a second test we have carried out a calculation using the model potential MOs, which are approximate eigenfunctions of the Hamiltonian (15) and (16); since they are written in terms of elliptic coordinates, it is appropriate to employ the CTF of Harel and Jouin [27]. It can be noted in Fig. 5 that the resulting cross section differs from the *ab initio* one at low energies, where the model potential treatment is probably less accurate; however, *ab initio* and model potential calculations with the 7MO basis set yield the same cross section at $E>1$ keV/amu, where the differences between *ab initio* and model potential are less important. This point is further illustrated in Fig. 6(c).

Our results for n-resolved cross sections are shown in Fig. 7. The 7MO basis is sufficient to obtain converged $n=2$ capture and excitation cross sections up to $E\sim 1$ keV/amu. Fur-

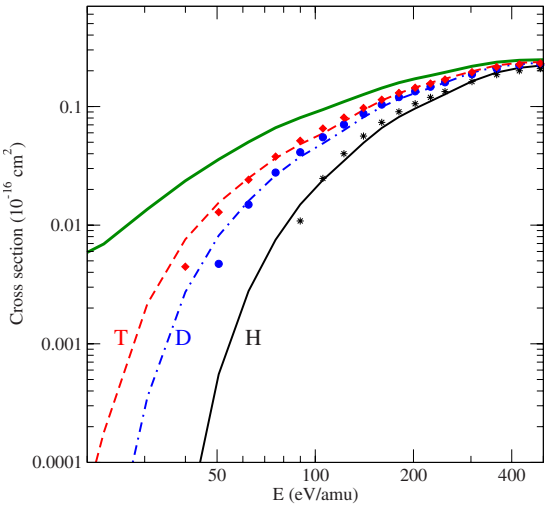

FIG. 8. (Color online) Cross sections for charge transfer in Li^++H (D, T) (1*s*) collisions. Thick line, eikonal calculation. Thin lines, quantal results for the different H isotopes as indicated in the figure. Symbols, results obtained by applying the Coulomb trajectory model of Eq. (21).

thermore, the quantal and semiclassical $n=2$ cross sections merge over a broad energy region, from $E\sim 0.5$ keV/amu to 1 keV/amu. The $n=3$ cross sections are found to be one order of magnitude smaller than the $n=2$ ones and the effects of v^2 terms and the eikonal approximation acquires greater importance so the merging of quantal and semiclassical results is less satisfactory than for $n=2$.

C. Isotope effect

To analyze the isotopic dependence of the CT cross section of reaction (1), we plot in Fig. 8 the CT total cross section for reaction (1) at low energies. As expected, we can observe that this cross section increases as μ increases, approaching the eikonal result. The energy dependence of the cross section can be approximated by means of a simple semiclassical model; in this model the nuclei follow Coulomb trajectories, and electronic transitions only take place when an internuclear distance R_0 in the neighborhood of the 1–2 avoided crossing, is reached. For a given velocity v the maximum impact parameter b_m that fulfills this condition is

$$b_m^2 = R_0^2 - \frac{2q}{\mu v^2} R_0. \tag{19}$$

As an additional simplification, we assume that the transition probability is independent of b in the range $[0, b_m]$, yielding

$$\sigma(v) \approx 2\pi \int_0^{b_m} bP(v)db \approx \pi b_m^2 P(v) = \pi P(v) R_0^2 \left[1 - \frac{2q}{\mu v^2 R_0}\right] \tag{20}$$

which has a threshold at $v_t = \sqrt{\frac{2q}{\mu R_0}}$ for each μ. Within this approximation, we can identify the eikonal result $\sigma^{\text{eik}}(v)$ with the limit of Eq. (20) as $\mu \to \infty$, leading to

$$\sigma(v) \approx \sigma^{\text{eik}}(v)\left[1 - \frac{2q}{\mu v^2 R_0}\right]. \tag{21}$$

We have evaluated this expression with $q=1$ that corresponds to $H^+ - Li^+$ interaction and $R_0 = 0.4a_0$ and the results are displayed in Fig. 8. The good agreement with the quantal calculation indicates that the isotopic dependence is a kinematic effect for $v > v_t$. At lower energies, the model is not useful since the simple Coulomb trajectory is not appropriate and tunneling starts to be sizeable.

V. CONCLUSIONS

In this work we have evaluated partial and total cross sections for Li^++H(1*s*) collisions [reactions (1) and (2)] in the range of energies 25 eV/amu $< E <$ 2.5 keV/amu that we believe can be useful in future studies on fusion plasmas, since lithium is used in some fusion devices either for diagnostics or to reduce the sputtering from the reactor walls, and there are no previous data for these reactions at energies $E < 5$ keV/amu. Our calculation has been carried out by employing a basis set of *ab initio* molecular functions, and we have explicitly checked the workings of commonly used effective potentials. We have also calculated charge-transfer cross sections in Li($1s^2 2s$)+H^+ collisions [reaction (3)]. The main differences with previous calculations are that we have used *ab initio* molecular functions and applied a quantal formalism to evaluate the cross sections at low energies. Comparison with previous data for this reaction has allowed us to check the convergence of our close-coupling calculation. Our study points out that our basis set yields accurate cross sections up to $E=2.5$ keV/amu, where the levels Li ($n=4$) (not included in our basis) start to be populated, and this is a conservative limit for reactions (1) and (2).

We have presented quantal and semiclassical (eikonal) results, which overlap at relatively high energies (300 eV/amu), because trajectory effects are very important in Li^++H collisions. Given the relevance in fusion plasmas of reactions involving D and T, we have also calculated cross sections for $Li^+ - D$, T collisions. We have found that the isotope dependence obtained in the quantal calculation can be qualitatively explained as due to a simple kinematic effect.

ACKNOWLEDGMENTS

This work was partially supported by DGICYT Project No. ENE2004-06266 and No. FIS2004-04145. F.G. acknowledges CIEMAT for additional financial support. We thank P.J. Salas for providing us with his data in tabulated form.

[1] M. Apicella, G. Mazzitelli, V. P. Ridolfini, V. Lazarev, A. Alekseyev, A. Vertkov, and R. Zagorski, J. Nucl. Mater. **363-365**, 1346 (2007).
[2] V. A. Evtikhin, I. E. Lyublinski, A. V. Vertkov, S. V. Mirnov, and V. B. Lazarev, Fusion Eng. Des. **56-57**, 363 (2001).
[3] M. B. Shah, T. V. Goffe, and H. B. Gilbody, J. Phys. B **11**, L233 (1978).
[4] J. Schweinzer, R. Brandenburg, I. Bray, R. Hoekstra, F. Aumayr, R. K. Janev, and H. Winter, At. Data Nucl. Data Tables **72**, 239 (1999).
[5] R. Brandenburg, F. Aumayr, H. Winter, G. Petravich, S. Zoletnik, S. Fiedler, K. McCormick, and J. Schweinzer, Fusion Technol. **36**, 289 (1999).
[6] R. Schorn, E. Wolfrum, F. Aumayr, E. Hintz, D. Rusbuldt, and H. Winter, Nucl. Fusion **32**, 351 (1992).
[7] L. F. Errea, F. Guzmán, C. Illescas, L. Méndez, B. Pons, A. Riera, and J. Suárez, Plasma Phys. Controlled Fusion **48**, 1585 (2006).
[8] P. C. Stancil and B. Zygelman, Phys. Rev. Lett. **75**, 1495 (1995).
[9] B. H. Bransden and M. H. C. McDowell, *Charge Exchange and the Theory of Ion-Atom Collisions* (Clarendon, Oxford, 1992).
[10] S. B. Schneiderman and A. Russek, Phys. Rev. **181**, 311 (1969).
[11] W. R. Thorson and J. B. Delos, Phys. Rev. A **18**, 135 (1978).
[12] L. F. Errea, L. Méndez, and A. Riera, J. Phys. B **15**, 101 (1982).
[13] P. Barragán, L. F. Errea, L. Méndez, A. Macías, I. Rabadán, and A. Riera, Phys. Rev. A **70**, 022707 (2004).
[14] E. R. Davidson, in *MOTECC, Modern Techniques in Computational Chemistry*, edited by E. Clementi (ESCOM, Leiden, 1990).
[15] Y. Ralchenko, F.-C. Jou, D. Kelleher, A. Kramida, A. Musgrove, J. Reader, W. Wiese, and K. Olsen, NIST Atomic Spectra Database (Version 3.1.3), http://physics.nist.gov/asd3, National Institute of Standards and Technology, Gaithersburg, MD, 2007.
[16] R. J. Allan, A. S. Dickinson, and R. McCarroll, J. Phys B **16**, 467 (1983).
[17] J. P. Salas, J. Phys. B **33**, 3201 (2000).
[18] M. Klapisch, Comput. Phys. Commun. **2**, 239 (1971).
[19] J. F. Castillo, L. F. Errea, A. Macías, L. Méndez, and A. Riera, J. Chem. Phys. **103**, 2113 (1995).
[20] S. L. Varghese, W. Waggoner, and C. L. Cocke, Phys. Rev. A **29**, 2453 (1984).
[21] W. Fritsch and C. D. Lin, J. Phys. B **16**, 1595 (1983).
[22] R. D. DuBois, Phys. Rev. A **32**, 3319 (1985).
[23] L. F. Errea, C. Harel, H. Jouin, L. Méndez, B. Pons, and A. Riera, J. Phys. B **31**, 3527 (1998).
[24] L. F. Errea, L. Méndez, and A. Riera, Phys. Rev. A **27**, 3357 (1983).
[25] L. F. Errea, L. Méndez, and A. Riera, Z. Phys. D **14**, 229 (1989).
[26] A. Riera, Phys. Rev. A **30**, 2304 (1984).
[27] C. Harel and H. Jouin, J. Phys. B **25**, 221 (1992).
[28] The exponents α of the Cartesian Gaussian functions $x_O^n y_O^m z_O^l e^{-\alpha r_O^2}$ and the contraction coefficients are available on the website http://tcam.qui.uam.es/publicaciones/LiHbasis.html